JOURNAL OF MODERN OPTICS
2019, VOL. 66, NO. 20, 2043–2051
https://doi.org/10.1080/09500340.2019.1690712

Taylor & Francis
Taylor & Francis Group

Check for updates

Electric dipole power emission near an ENZ medium

Zhangjin Xu and Henk F. Arnoldus

Department of Physics and Astronomy, Mississippi State University, Mississippi State, MS, USA

ABSTRACT

Power emission by an electric dipole near an interface is considered. We derive explicit expressions for the emitted power for any state of oscillation of the dipole, without making use of the material properties of the substrate, and we derive an expression for the power crossing the interface. It is shown that the power naturally splits in contributions from travelling and evanescent incident waves. Only the part with the evanescent waves contributes to the transmitted power. We then consider an epsilon-equal-zero material and obtain explicit expressions for the power. It is shown that only travelling waves contribute, and that no power crosses into the material. When the slightest amount of absorption is present in the medium, the evanescent waves kick in, and in such a way that the emitted power diverges when the distance between the dipole and the interface becomes small.

ARTICLE HISTORY
Received 16 October 2019
Accepted 1 November 2019

KEYWORDS
ENZ material; dipole radiation; dipole power; interface

1. Introduction

A particle with an oscillating electric dipole moment will emit electromagnetic radiation. The energy emission rate of the particle is not only determined by the state of oscillation of the dipole moment, but also by its environment. Reflected radiation by, for instance, a nearby interface, influences the emission rate. Such alterations of the emission rate have been observed experimentally for Rydberg atoms in a cavity (*1*) and in between parallel mirrors (*2*). Similarly, the fluorescence emission rate of molecules near a substrate is affected by the material, as was experimentally confirmed in the celebrated experiments by Drexhage (*3*). Numerous theoretical approaches have been presented (*4,5*). The angular spectrum approach (*6,7*) is based on Weyl's representation of the scalar Green's function, but also Sommerfeld's representation, involving a Bessel function, is widely used (*8,9*). Theoretical predictions have been verified experimentally for dipoles near a conducting surface (*10,11*), and extensions to wave guide structures have been studied (*12*). For atoms, molecules, nano- and microparticles, the electric dipole moment will provide the dominant mode of radiation. When such a small particle is irradiated by a laser beam of angular frequency ω, an electric dipole moment will be induced. With $\boldsymbol{d}$ the complex amplitude of the oscillating dipole moment, the emitted power is given by (*13*)

$$P_{\rm o} = \frac{\omega^4}{12\pi\varepsilon_{\rm o}c^3}\boldsymbol{d}^*\cdot\boldsymbol{d}, \tag{1}$$

when the particle is surrounded by free space only. We shall set $\boldsymbol{d} = d_{\rm o}\hat{\boldsymbol{u}}$, with $d_{\rm o} > 0$ and $\hat{\boldsymbol{u}}^*\cdot\hat{\boldsymbol{u}} = 1$. Then the amplitude $d_{\rm o}$ is determined by the laser power, and the polarization $\hat{\boldsymbol{u}}$ of the dipole moment is determined by the polarization of the laser electric field. When $\hat{\boldsymbol{u}}$ is real, apart from a possible overall phase factor, the oscillation is linear. When $\hat{\boldsymbol{u}}$ is complex, the dipole moment rotates, and traces out an ellipse in a plane.

In general, the time-averaged emitted power by an oscillating electric dipole is given by (*14*)

$$P = \tfrac{1}{2}\omega{\rm Im}[\boldsymbol{d}^*\cdot\boldsymbol{E}(\boldsymbol{r}_{\rm o})], \tag{2}$$

with $\boldsymbol{E}(\boldsymbol{r}_{\rm o})$ the complex amplitude of the electric field at the location $\boldsymbol{r}_{\rm o}$ of the dipole. This field is the field by the dipole itself, the source field, and, for instance, the field reflected by an interface. If we only consider the source field, expression (2) reduces to $P_{\rm o}$ from Equation (1) (*14*). When the particle is located near an interface, the reflected electric field adds to $\boldsymbol{E}(\boldsymbol{r}_{\rm o})$, and the power acquires an additional term due to the reflected field.

We shall consider the power emitted by an electric dipole near the surface of an epsilon-near-zero (ENZ) material. Such materials are usually metamaterials. These

CONTACT Henk F. Arnoldus hfa1@msstate.edu Department of Physics and Astronomy, Mississippi State University, P.O. Box 5167, Mississippi State, MS 39762, USA

© 2019 Informa UK Limited, trading as Taylor & Francis Group

artificial media are sub-wavelength structures that effectively act as a continuum for the frequency range under consideration. By tailoring the structures, in principal any values of the (relative) permittivity ε and (relative) permeability μ can be obtained. However, such media also occur naturally in nature. For instance, a metal near the plasmon resonance has a permittivity with a real part almost zero, and a small imaginary part. The permittivity is a function of the frequency, and this leads to dispersion of a wave packet or pulse. This is the basis for the generation of slow light. For the present problem, we consider a dipole oscillating at a single frequency. An ENZ medium is a material with $\varepsilon \approx 0$ and $\mu = 1$. The first demonstrations of metamaterial ENZ media were in the microwave and terahertz regions (*15–19*), and later ENZ materials for the visible part of the spectrum were constructed (*20–22*). ENZ materials are nearly impenetrable for radiation. When a plane wave is incident upon the interface, the wave in the material is evanescent, and does not propagate into the medium (*23*). An exception is when the wave is under (near) normal incidence. Then an oscillating electric field penetrates the material, but it has no spatial dependence. This phenomenon is called 'static optics'. It can be used for letting radiation tunnel (or funnel) through the material without loss of phase information (*24–29*). It also allows for the construction of an angular filter (*30–33*). Another prediction is that the force between the dipole and the ENZ surface is repulsive (*34–37*), leading to possible levitation of the particle. A line source near an epsilon-near-zero metamaterial interface has been predicted to produce a strongly directed beam (*38*), and epsilon-near zero substrates have been shown to significantly enhance second harmonic generation (*39*), as compared to ordinary dielectrics or metals. We shall show that the presence of an ENZ interface greatly affects the power emission rate. An interesting aspect of this problem is that it can be solved analytically, whereas for other media one has to resort to a numerical approach.

2. Electric dipole near an interface

We first consider the more general case of an electric dipole located a distance H away from the interface with a material, as illustrated in Figure 1. The dipole is located on the z-axis, and we take the surface as the xy plane. The dipole is embedded in a medium with permittivity ε_1 and permeability μ_1, both assumed to be positive That assumption is not really a necessary restriction at this point, but we shall see below that it provides a huge computational advantage. The index of refraction is then $n_1 = (\varepsilon_1\mu_1)^{1/2}$. The medium can be a half-infinite material, or a more complicated stratified structure. We shall

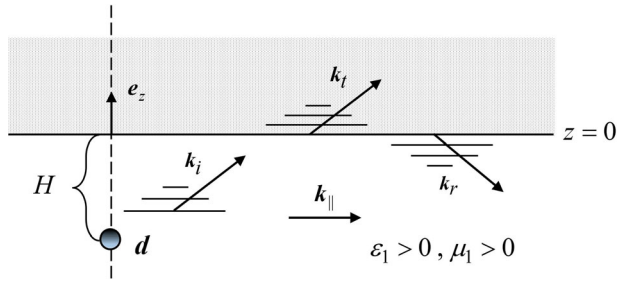

Figure 1. The figure shows schematically the setup under consideration. The dipole is located a distance H below an interface with a material medium. Partial waves in the angular spectrum can be travelling, indicated by arrows, or evanescent in the z-direction, indicated by dashed lines. Due to boundary conditions, each wave vector must have the same parallel component $\boldsymbol{k}_{||}$. The transmitted wave vector shown is for a semi-infinite medium, but that is only for illustration.

for now only assume that the reflection of a plane wave can be accounted for by the Fresnel reflection coefficients R_s and R_p for s and p polarized radiation, respectively.

The electric field, emitted by the dipole, is the source field, and it can be represented by an angular spectrum of plane waves. We have (*40*)

$$\boldsymbol{E}_s(\boldsymbol{r}) = \frac{i\mu_1 k_o d_o}{8\pi^2\varepsilon_o}\sum_{\sigma=s,p}\int \mathrm{d}^2\boldsymbol{k}_{||}\frac{e^{i\boldsymbol{k}_{||}\cdot\boldsymbol{r}}}{v_1} \times (\hat{\boldsymbol{u}}\cdot\boldsymbol{e}_{\sigma,i})\boldsymbol{e}_{\sigma,i}e^{iv_1(h+k_o z)}\,,\ -H < z < 0. \quad (3)$$

We have set $h = k_o H$ for the dimensionless distance between the particle and the surface. For each $\boldsymbol{k}_{||}$ this is a plane wave, and the integral runs over the $\boldsymbol{k}_{||}$ plane, which is the xy plane. The wave vector of a partial wave is $\boldsymbol{k}_i = \boldsymbol{k}_{||} + k_o v_1 \boldsymbol{e}_z$, and these waves are the incident plane waves on the surface. Here, v_1 is the dimensionless z component of the wave vector. First, we set

$$\alpha = \frac{k_{||}}{k_o}, \quad (4)$$

for the dimensionless magnitude of $\boldsymbol{k}_{||}$. From the dispersion relation it then follows that

$$v_1 = \begin{cases} \sqrt{n_1^2 - \alpha^2}, 0 \le \alpha < n_1 \\ i\sqrt{\alpha^2 - n_1^2}, n_1 < \alpha < \infty \end{cases}. \quad (5)$$

For $\alpha < n_1$, the z component of the incident wave vector is real, and the plane wave is a travelling wave. With θ_i the angle of incidence, we have $\alpha = n_1 \sin\theta_i$. For $\alpha > n_1$, the z component of the incident wave is positive imaginary, and the wave decays exponentially in the positive z-direction, which is the direction towards the surface. These are the evanescent waves of the incident field. This is schematically depicted in Figure 1. For $\alpha = 0$, we

have normal incidence, and for $\alpha \lesssim n_1$ we have grazing incidence. Borderline is $\alpha = n_1$, for which $\nu_1 = 0$. We then get a division by zero on the right-hand side of Equation (3). We shall see below that this singularity is integrable, and can be transformed away by a proper change of variables. The polarization vectors of an incident wave are

$$\boldsymbol{e}_{s,i} = \boldsymbol{e}_z \times \hat{\boldsymbol{k}}_{||}, \tag{6}$$

$$\boldsymbol{e}_{p,i} = \frac{1}{n_1}(\alpha \boldsymbol{e}_z - \nu_1 \hat{\boldsymbol{k}}_{||}), \tag{7}$$

given $\hat{\boldsymbol{k}}_{||} = \boldsymbol{k}_{||}/k_{||}$, the unit vector in the $\boldsymbol{k}_{||}$ direction. The corresponding magnetic field follows, in general, from the electric field as <script type="math/tex; mode=display" id="MathJax-Element-46">

$$\boldsymbol{B}(\boldsymbol{r}) = -\frac{i}{\omega}\nabla \times \boldsymbol{E}(\boldsymbol{r}). \tag{8}$$

</script>The field from Equation (3), together with the corresponding magnetic field, is the incident field on the interface. The reflection of each partial wave can be accounted for by a Fresnel reflection coefficient. We thus find the angular spectrum of the reflected electric field to be

$$\boldsymbol{E}_r(\boldsymbol{r}) = \frac{i\mu_1 k_0 d_0}{8\pi^2 \varepsilon_0} \sum_{\sigma=s,p} \int \mathrm{d}^2\boldsymbol{k}_{||} \frac{e^{i\boldsymbol{k}_{||}\cdot\boldsymbol{r}}}{\nu_1} \times (\hat{\boldsymbol{u}} \cdot \boldsymbol{e}_{\sigma,i})\boldsymbol{e}_{\sigma,r} R_\sigma e^{i\nu_1(h-k_0 z)}, \; z < 0. \tag{9}$$

The wave vector of a partial reflected wave is $\boldsymbol{k}_r = \boldsymbol{k}_{||} - k_0\nu_1\boldsymbol{e}_z$, which only differs from $\boldsymbol{k}_i$ in the sign of its z component. If the incident wave is travelling, then so is the reflected wave. When the incident wave is evanescent, so is the reflected wave, but this wave decays into the direction away from the surface, as it should be. The polarization vector $\boldsymbol{e}_{s,r}$ is the same as $\boldsymbol{e}_{s,i}$ from Equation (6). For p polarization, vector $\boldsymbol{e}_{p,r}$ follows from Equation (7) by replacing ν_1 by $-\nu_1$. The reflected magnetic field follows from $\boldsymbol{E}_r(\boldsymbol{r})$ as in Equation (8).

3. Power emission

The emitted power by the dipole is given by Equation (2), with $\boldsymbol{E}(\boldsymbol{r}_0) = \boldsymbol{E}_s(\boldsymbol{r}_0) + \boldsymbol{E}_r(\boldsymbol{r}_0)$, and $\boldsymbol{r}_0 = -H\boldsymbol{e}_z$. For the power, we write

$$P = P_s + P_r, \tag{10}$$

in obvious notation. The power due to the source field cannot be directly computed from the expression for $\boldsymbol{E}_s(\boldsymbol{r})$ in Equation (3), since this expression only holds for $-H < z < 0$. A much simpler approach is given in Ref. (*14*). We then immediately find

$$P_s = \mu_1 n_1 P_0, \tag{11}$$

with P_0 the emitted power in free space (Equation 1). The embedding medium gives an extra factor of $\mu_1 n_1$.

To compute P_r, we set $\boldsymbol{r}_0 = -H\boldsymbol{e}_z$ in Equation (9). An immediate simplification is that $\exp(i\boldsymbol{k}_{||} \cdot \boldsymbol{r}_0) = 0$. We then adopt polar coordinates $(\boldsymbol{k}_{||}, \hat{\phi})$ in the $\boldsymbol{k}_{||}$ plane, and we change variables from $k_{||}$ to α as in Equation (4). We then have $\hat{\boldsymbol{k}}_{||} = \boldsymbol{e}_x \cos\hat{\phi} + \boldsymbol{e}_y \sin\hat{\phi}$, and the polarization vectors can be expressed in terms of α and $\hat{\phi}$. The Fresnel coefficients only depend on α. The integrals over $\hat{\phi}$ are then elementary. We split the dipole moment polarization vector $\hat{\boldsymbol{u}}$ in its perpendicular and parallel components with respect to the surface:

$$\hat{\boldsymbol{u}} = \hat{\boldsymbol{u}}_\perp + \hat{\boldsymbol{u}}_{||}. \tag{12}$$

We then obtain for the emitted power

$$P = \mu_1 n_1 P_0[(\hat{\boldsymbol{u}}_\perp^* \cdot \hat{\boldsymbol{u}}_\perp) w_\perp(h) + (\hat{\boldsymbol{u}}_{||}^* \cdot \hat{\boldsymbol{u}}_{||}) w_{||}(h)]. \tag{13}$$

This expression involves the two functions

$$w_\perp(h) = 1 + \frac{3}{2n_1^3}\mathrm{Re}\int_0^\infty \mathrm{d}\alpha \frac{\alpha^3}{\nu_1} e^{2ih\nu_1} R_p(\alpha), \tag{14}$$

$$w_{||}(h) = 1 + \frac{3}{4n_1^3}\mathrm{Re}\int_0^\infty \mathrm{d}\alpha \frac{\alpha}{\nu_1} e^{2ih\nu_1} \times [n_1^2 R_s(\alpha) - \nu_1^2 R_p(\alpha)]. \tag{15}$$

The attractive result (13–15) holds for any dipole polarization $\hat{\boldsymbol{u}}$, and no use has been made of any properties of the reflection coefficients (apart from the fact that they are rotationally symmetric around the z-axis, so they only depend on α). The terms '1' on the right-hand sides give P_s from Equation (11), since $\hat{\boldsymbol{u}}_\perp^* \cdot \hat{\boldsymbol{u}}_\perp + \hat{\boldsymbol{u}}_{||}^* \cdot \hat{\boldsymbol{u}}_{||} = 1$.

4. Travelling and evanescent contributions

The integration range $0 \le \alpha < n_1$ in Equations (14) and (15) represents the contribution from the travelling incident waves in the angular spectrum. Similarly, the range $n_1 < \alpha < \infty$ accounts for the evanescent dipole waves. We split the functions accordingly:

$$w_\gamma(h) = 1 + w_\gamma(h)^{tr} + w_\gamma(h)^{ev}, \quad \gamma = \perp, \; ||. \tag{16}$$

For the travelling parts, we make the substitution, similar as in Ref. (*38*):

$$n_1 u = \sqrt{n_1^2 - \alpha^2} \quad (tr) \tag{17}$$

This yields the new representations

$$w_\perp(h)^{tr} = \frac{3}{2}\mathrm{Re}\int_0^1 \mathrm{d}u\, e^{i\beta u}(1-u^2)R_p, \tag{18}$$

$$w_{||}(h)^{tr} = \frac{3}{4}\mathrm{Re}\int_0^1 \mathrm{d}u\, e^{i\beta u}(R_s - u^2 R_p). \tag{19}$$

Here we introduced

$$\beta = 2n_1 h, \tag{20}$$

and the dependence on h only enters through β. As compared to Equations (14) and (15), the $1/\nu_1$ singularity has disappeared, and so has the ν_1 in the exponent. The Fresnel coefficients are now evaluated at

$$\alpha = n_1\sqrt{1-u^2} \quad (tr). \tag{21}$$

For the evanescent contributions, we set

$$n_1 u = \sqrt{\alpha^2 - n_1^2} \quad (ev), \tag{22}$$

so that for the Fresnel coefficients we need to take

$$\alpha = n_1\sqrt{1+u^2} \quad (ev). \tag{23}$$

We then obtain the new representations

$$w_\perp(h)^{ev} = \frac{3}{2}\int_0^\infty \mathrm{d}u\, e^{-\beta u}(1+u^2)\mathrm{Im}R_p, \tag{24}$$

$$w_{||}(h)^{ev} = \frac{3}{4}\int_0^\infty \mathrm{d}u\, e^{-\beta u}\mathrm{Im}(R_s + u^2 R_p). \tag{25}$$

Interestingly, only the imaginary parts of the Fresnel coefficients come into these representations. We will see the significance of this for ENZ media in Section 9.

It is worthwhile noticing that the clean splitting in $tr + ev$ is a result of our assumption that there is no damping in the embedding medium. If ε_1 or μ_1 would have an imaginary part, then n_1 would be complex, and so it would not be on the line of integration. Furthermore, we shall see in the next section that the travelling and evanescent parts of the emitted power have distinct physical interpretations.

5. Power through the interface

Conservation of energy implies that the emitted power P by the dipole either radiates away into the region $z < 0$, where it ends up in the far field, or it passes through the surface. We shall write

$$P = P_\perp + P_1, \tag{26}$$

and here $P_\perp$ represents the part that crosses the interface, whereas P_1 is the part that propagates to the far field in medium 1. In this section, we derive an expression for $P_\perp$, without any assumptions yet about the material of the medium.

The flow of energy is accounted for by the time-averaged Poynting vector $\boldsymbol{S}(\boldsymbol{r})$. In the embedding medium, the region $z < 0$, this vector is

$$\boldsymbol{S}(\boldsymbol{r}) = \frac{1}{2\mu_\mathrm{o}\mu_1}\mathrm{Re}[\boldsymbol{E}(\boldsymbol{r})^* \times \boldsymbol{B}(\boldsymbol{r})]. \tag{27}$$

The power passing through the surface $z = 0$ is then

$$P_\perp = \int_{xy\,\mathrm{plane}} \boldsymbol{S}(x,y,0)\cdot\boldsymbol{e}_z\,\mathrm{d}A. \tag{28}$$

With a vector identity this can be written as

$$P_\perp = \frac{1}{2\mu_o\mu_1}\mathrm{Re}\int_{xy\,\mathrm{plane}} \boldsymbol{E}(x,y,0)^*\cdot[\boldsymbol{B}(x,y,0)\times\boldsymbol{e}_z]\mathrm{d}A. \tag{29}$$

Both the electric and the magnetic fields are the sums of the source field and the reflected field. With Equations (3) and (9) we find

$$\boldsymbol{E}(x,y,0) = \frac{i\mu_1 k_\mathrm{o} d_\mathrm{o}}{8\pi^2\varepsilon_\mathrm{o}}\sum_{\sigma=s,p}\int \mathrm{d}^2\boldsymbol{k}_{||}\frac{e^{i\boldsymbol{k}_{||}\cdot\boldsymbol{r}}}{\nu_1}e^{i\nu_1 h} \times(\hat{\boldsymbol{u}}\cdot\boldsymbol{e}_{\sigma,i})[\boldsymbol{e}_{\sigma,i} + R_\sigma(\alpha)\boldsymbol{e}_{\sigma,r}]. \tag{30}$$

The magnetic field follows from Equation (8), and after working out the cross products between $\boldsymbol{e}_z$ and the polarization vectors we find

$$\boldsymbol{B}(x,y,0)\times\boldsymbol{e}_z = \frac{i\mu_1 k_\mathrm{o} d_\mathrm{o}}{8\pi^2\varepsilon_\mathrm{o}}\frac{n_1}{c}\int \mathrm{d}^2\boldsymbol{k}_{||}\frac{e^{i\boldsymbol{k}_{||}\cdot\boldsymbol{r}}}{\nu_1}e^{i\nu_1 h} \times\left\{\frac{\nu_1}{n_1}(\hat{\boldsymbol{u}}\cdot\boldsymbol{e}_{s,i})[1-R_s(\alpha)]\boldsymbol{e}_{s,i} - (\hat{\boldsymbol{u}}\cdot\boldsymbol{e}_{p,i})[1+R_p(\alpha)]\hat{\boldsymbol{k}}_{||}\right\}. \tag{31}$$

The right-hand sides of Equations (30) and (31) are then substituted into Equation (9). We are then left with a product of two angular spectra, which may seem daunting. However, the dependence on x and y only enters through the exponentials $\exp(i\boldsymbol{k}_{||}\cdot\boldsymbol{r})$, and orthogonality comes to the rescue:

$$\int_{xy\,\mathrm{plane}} e^{i(\boldsymbol{k}_{||}-\boldsymbol{k}_{||}')\cdot\boldsymbol{r}}\mathrm{d}A = 4\pi^2\delta(\boldsymbol{k}_{||}-\boldsymbol{k}_{||}'). \tag{32}$$

When integrated over the xy plane, there is no coupling between different $\boldsymbol{k}_{||}$ modes of $\boldsymbol{E}$ and $\boldsymbol{B}$. As in Section 3, we adopt polar coordinates $(\boldsymbol{k}_{||},\hat{\phi})$ in the $\boldsymbol{k}_{||}$ plane. The $\hat{\phi}$ dependence only enters through the various polarization

vector, and the integrations over $\hat{\phi}$ are easy. The result simplifies considerably:

$$P_\perp = \frac{3\mu_1}{8n_1^2}P_o\mathrm{Re}\int_0^\infty d\alpha\frac{\alpha}{\nu_1}e^{-2h\mathrm{Im}\nu_1}\{n_1^2[1+R_s(\alpha)]\times[1-R_s(\alpha)^*](\hat{\boldsymbol{u}}_{||}^*\cdot\hat{\boldsymbol{u}}_{||})+[1+R_p(\alpha)]\times[1-R_p(\alpha)^*][\nu_1^2(\hat{\boldsymbol{u}}_{||}^*\cdot\hat{\boldsymbol{u}}_{||})+2\alpha^2(\hat{\boldsymbol{u}}_\perp^*\cdot\hat{\boldsymbol{u}}_\perp)]\}. \quad (33)$$

At this point, it is advantageous to split the α integral in its travelling and evanescent parts. We make use of the fact that ν_1 is real for travelling waves and imaginary for evanescent waves, as shown in Equation (5). After some regrouping, we finally obtain

$$P_\perp = \mu_1 n_1 P_o\left\{\tfrac{1}{2}+(\hat{\boldsymbol{u}}_\perp^*\cdot\hat{\boldsymbol{u}}_\perp)[w_\perp(h)^{ev}-z_\perp]+(\hat{\boldsymbol{u}}_{||}^*\cdot\hat{\boldsymbol{u}}_{||})[w_{||}(h)^{ev}-z_{||}]\right\}. \quad (34)$$

Here we introduced the functions

$$z_\perp = \frac{3}{4n_1^3}\int_0^{n_1} d\alpha\frac{\alpha^3}{\nu_1}|R_p(\alpha)|^2, \quad (35)$$

$$z_{||} = \frac{3}{8n_1^3}\int_0^{n_1} d\alpha\frac{\alpha}{\nu_1}[n_1^2|R_s(\alpha)|^2+\nu_1^2|R_p(\alpha)|^2]. \quad (36)$$

The result (34) has an interesting interpretation. The ½ gives half of P_s from Equation (11). This term represents the fact that half the radiation that would be emitted without the interface is emitted towards the interface. The terms with $z_\perp$ and $z_{||}$ represent the part that is reflected back into the region $z < 0$. They give a negative contribution, and they only depend on the absolute value of the Fresnel reflection coefficients. These functions are independent of h, and they only contain travelling waves, as can be seen from the integration limits. The functions $w_\perp$ and $w_{||}$ represent interference between source waves and reflected waves. Oddly enough, only the evanescent parts of these functions contribute to the transmission of power through the interface. This also implies that the travelling parts of these functions represent emitted power that travels directly to the far field in $z < 0$.

For the functions $z_\perp$ and $z_{||}$ we can make the same change of variables as in Equation (17). This yields the simpler-looking forms

$$z_\perp = \frac{3}{4}\int_0^1 du(1-u^2)|R_p|^2, \quad (37)$$

$$z_{||} = \frac{3}{8}\int_0^1 du(|R_s|^2+u^2|R_p|^2). \quad (38)$$

The Fresnel coefficients are here evaluated at α from Equation (21).

6. Emitted power near an $\varepsilon = 0$ medium

We now consider the case where the medium is an $\varepsilon = 0$ material. We then have $\varepsilon = 0$, $\mu = 1$, and we shall also assume $\mu_1 = 1$ for the embedding medium. The Fresnel reflection coefficients for such a medium are (*23*)

$$R_s(\alpha) = \frac{1}{n_1^2}(\nu_1 - i\alpha)^2, \quad (39)$$

$$R_p(\alpha) = -1, \quad (40)$$

with ν_1 given by Equation (5). For a travelling wave, we have $\alpha = n_1\sin\theta_i$, with θ_i the angle of incidence. Then $\nu_1 = n_1\cos\theta_i$, and $\nu_1 - i\alpha = n_1\exp(-i\theta_i)$. Therefore

$$R_s(\alpha) = e^{-2i\theta_i} \quad (tr), \quad (41)$$

and we have $|R_s(\alpha)| = 1$. For evanescent waves, $R_s(\alpha)$ is real and limited by

$$-1 < R_s(\alpha) < 0 \quad (ev). \quad (42)$$

Figure 2 represents $R_s(\alpha)$ pictorially in the complex plane.

For evanescent waves, R_s and R_p are real, and with Equations (24) and (25) we immediately find

$$w_\perp(h)^{ev} = w_{||}(h)^{ev} = 0. \quad (43)$$

Evanescent waves do not contribute to the emitted power. With $R_p = -1$, the integral in Equation (18) can be computed, and we find

$$w_\perp(h) = 1 + \frac{3}{\beta^2}\left(\cos\beta - \frac{1}{\beta}\sin\beta\right). \quad (44)$$

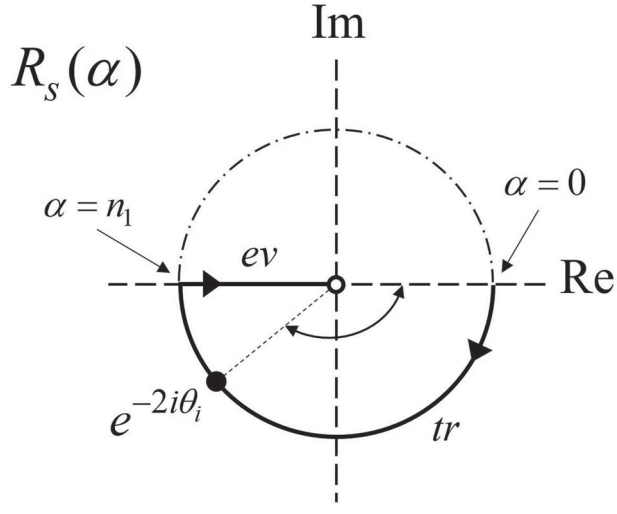

Figure 2. Shown is the reflection coefficient for *s* waves. For travelling waves, $R_s(\alpha)$ lies on the unit circle, and its phase angle is twice the angle of incidence, measured clockwise. For evanescent waves, $R_s(\alpha)$ is negative.

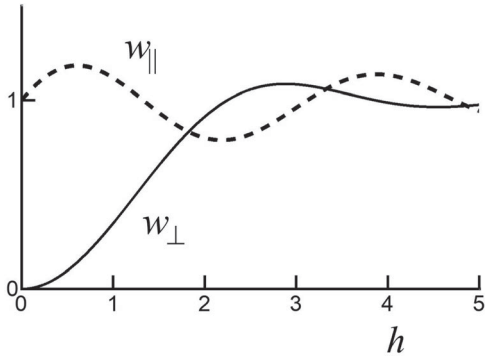

Figure 3. The figure shows the two functions that determine the power emission near an ENZ interface, for $n_1 = 1$.

For the integral in Equation (19), we use Equation (39) for R_s, and we then obtain

$$w_{||}(h) = 1 + \frac{3}{2\beta}\left[\sin\beta + \frac{3}{\beta}\left(\cos\beta - \frac{1}{\beta}\sin\beta\right)\right] + \frac{3\pi}{4\beta}J_2(\beta), \tag{45}$$

with $J_2(\beta)$ a Bessel function. Expressions (44) and (45) are parameter free functions of β, and the graphs are shown in Figure 3 as a function of h. Both $w_\perp(h)$ and $w_{||}(h)$ level off to unity for h large, as it should be, since for h large the effect of the interface should disappear.

7. Behaviour for *h* small

Expressions (44) and (45) seem to have negative powers of β, which suggests that these functions diverge for β, or h, small. Figure 3, however, shows that the functions are finite for $h = 0$. In order to study the behaviour for β small, we set $R_p = -1$ in Equation (18), which gives

$$w_\perp(h)^{tr} = -\frac{3}{2}\int_0^1 \mathrm{d}u\,(1-u^2)\cos(\beta u). \tag{46}$$

Then we expand $\cos(\beta u)$ in a series, and integrate term-by-term. The first term in the series cancels the 1 on the right-hand side of Equation (16), and we find

$$w_\perp(h) = -6\sum_{k=1}^{\infty}\frac{k+1}{(2k+3)!}(-\beta^2)^k. \tag{47}$$

The first few terms are

$$w_\perp(h) = \tfrac{1}{10}\beta^2 - \tfrac{1}{280}\beta^4 + \ldots, \tag{48}$$

and in particular $w_\perp(0) = 0$. With some more effort, we find

$$w_{||}(h) = 1 + 6\sum_{k=1}^{\infty}\frac{k(k+1)}{(2k+3)!}(-\beta^2)^k + 3\pi\beta\sum_{k=0}^{\infty}\frac{1}{4^{k+2}k!(k+2)!}(-\beta^2)^k, \tag{49}$$

with the first few terms being

$$w_{||}(h) = 1 + \tfrac{3\pi}{32}\beta - \tfrac{1}{10}\beta^2 + \ldots, \tag{50}$$

from which $w_{||}(0) = 1$, as in the graph.

8. Power crossing the $\varepsilon = 0$ interface

An interesting question is whether any energy passes through the interface. The general expression for $P_\perp$ is given by Equation (34). We already found $w_\perp(h)^{ev} = w_{||}(h)^{ev} = 0$ for the $\varepsilon = 0$ medium, so it remains to find $z_\perp$ and $z_{||}$, defined by Equations (35) and (36). Only travelling waves contribute, and therefore we have $|R_s| = 1$ and $|R_p| = 1$. From the representations (37) and (38) we readily find

$$z_\perp = z_{||} = \tfrac{1}{2}, \tag{51}$$

and therefore

$$P_\perp = 0. \tag{52}$$

No energy is transferred through the interface into the $\varepsilon = 0$ material.

It should be noted, however, that this does not necessarily imply that no energy penetrates the material. It can very well be that energy crosses into the material locally, but then returns somewhere close by back to the region $z < 0$. Such sub-wavelength back-and-forth oscillations of energy have been predicted for a regular dielectric-dielectric interface when the medium is thinner than the embedding medium of the dipole (*41*). The fact that $P_\perp$ vanishes only implies that the net energy flow across the interface is zero.

9. Role of damping

A medium with ε exactly equal to zero is most likely not possible to construct with metamaterial technology. The functions $w_\perp(h)$ and $w_{||}(h)$ shown in Figure 3 are universal functions representing the power emission near an interface, with ε identically equal to zero. For arbitrary ε, these functions can be obtained by numerical integration of the representations given in Equations 18, 19, 24 and 25. A typical example of $w_\perp(h)$ is shown by the solid curve in Figure 4 for $\varepsilon = 0.1 * i$. The dashed curve is the

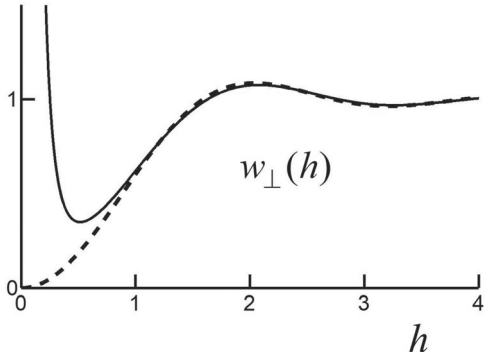

Figure 4. Shown is the function $w_\perp(h)$ for $\varepsilon = 0.1 * i$ (solid curve) and $\varepsilon = 0$ (dashed curve).

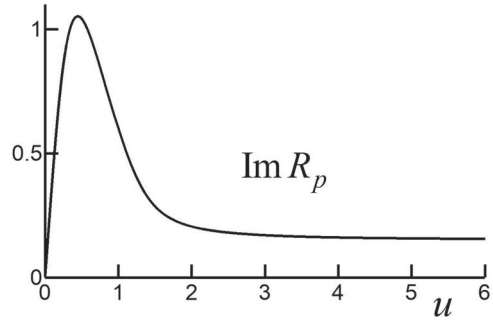

Figure 5. The graph shows the imaginary part of R_p as a function of u for $\varepsilon_1 = 2$ and $\varepsilon = 5 + 2 * i$.

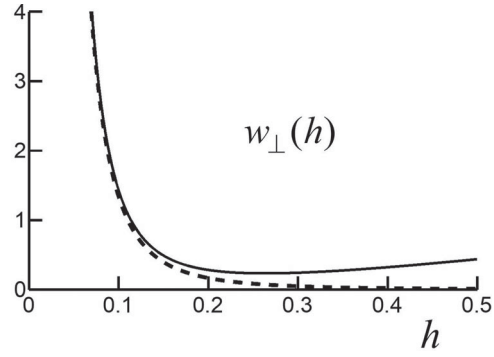

Figure 6. The graph illustrates that the approximation of $w_\perp(h)$ by the term shown on the right-hand side of Equation (58) is excellent at small distances.

same as the solid curve in Figure 3. The most striking feature is that $w_\perp(h)$ diverges for $h \to 0$ for $\varepsilon \neq 0$. For an ENZ material, ε is close to zero, but not exactly equal to zero. Apparently, this makes a big difference.

The travelling part of $w_\perp(h)$ is given by Equation (18). The integral is over a finite range, and is therefore finite. This implies that the diverging behaviour for h small has to come from the evanescent contribution from Equation (24). With ε the permittivity of the medium and ε_1 the permittivity of the embedding medium of the dipole, the Fresnel reflection coefficient for p waves is

$$R_p = \frac{\varepsilon \nu_1 - \varepsilon_1 \nu}{\varepsilon \nu_1 + \varepsilon_1 \nu}. \tag{53}$$

Here, ν_1 is given by Equation (5), and since we are considering the evanescent range, $\alpha > n_1$, this parameter is positive imaginary. The parameter ν is defined similarly

$$\nu = \sqrt{n^2 - \alpha^2}. \tag{54}$$

Here, $n = \sqrt{\varepsilon}$ is the index of refraction of the material, which is complex, in general. This ν is the dimensionless z component of the plane wave that is transmitted into the medium. For an $\varepsilon = 0$ material we have $\nu = i\alpha$, and this makes R_p real. Therefore, $\mathrm{Im}R_p = 0$, and $w_\perp(h)^{ev} = 0$.

Let us now consider what happens when $\varepsilon \neq 0$. In Equation (54), $\alpha > n_1$, since we are considering the region where the incident waves are evanescent. Assume first that ε is real and positive, like for an ordinary dielectric. If $\varepsilon < \varepsilon_1$, then $n < n_1$, and ν_1 is positive imaginary, since $\alpha > n_1$. Then the transmitted wave is evanescent, R_p is real, $\mathrm{Im}R_p = 0$, and $w_\perp(h)^{ev} = 0$. For $\varepsilon > \varepsilon_1$ we introduce the parameter

$$u_o = \sqrt{\frac{\varepsilon}{\varepsilon_1} - 1}, \tag{55}$$

which is positive. For $0 \leq u < u_o$ the transmitted wave is travelling, ν is real, $|R_p| = 1$, $\mathrm{Im}R_p \neq 0$. For $u > u_o$, the transmitted wave is evanescent, and $\mathrm{Im}R_p = 0$. So, in this case, the integral over u in Equation (24) runs to u_o, rather than infinity, and this gives a finite contribution to $w_\perp(h)^{ev}$.

Apparently, when $\varepsilon > 0$ the contribution of $w_\perp(h)^{ev}$ to $w_\perp(h)$ is either zero or finite. We now consider the situation where ε has a positive imaginary part, responsible for damping in the material. Then $\mathrm{Im}R_p \neq 0$ for all u, and the integral in Equation (24) runs to infinity. The part $u^2 \exp[-\beta u]$ of the integrand has a maximum at $u = 2/\beta$, and that maximum is $4/(e^2\beta^2)$. For β (and h) small, this maximum moves to high u values, and the peak height increases as $1/\beta^2$. This function is multiplied by $\mathrm{Im}R_p$. This function is shown in Figure 5 for $\varepsilon_1 = 2$ and $\varepsilon = 5 + 2 * i$. We see that $\mathrm{Im}R_p$ levels off to a constant, already for moderate values of u. Since $u^2 \exp[-\beta u]$ gives the main contribution from the region $u \sim 2/\beta$, we can replace $\mathrm{Im}R_p(u)$ by $\mathrm{Im}R_p(\infty)$ as a good approximation for β small. For u large, we have $\nu \approx \nu_1$, and we find with Equation (51)

$$R_p(\infty) = \frac{\varepsilon - \varepsilon_1}{\varepsilon + \varepsilon_1}. \tag{56}$$

Taking the imaginary part and using that ε is small then gives

$$\mathrm{Im}R_p(\infty) = \frac{2}{\varepsilon_1}\mathrm{Im}\varepsilon. \tag{57}$$

Then the integral in Equation (24) is easily computed. For $\mathrm{Im}\varepsilon \neq 0$ this is then the dominant term for β small. We thus obtain

$$w_\perp(h) = \frac{6}{\varepsilon_1\beta^3}\mathrm{Im}\varepsilon + \ldots, \tag{58}$$

and along similar lines we find

$$w_{||}(h) = \frac{3}{\varepsilon_1\beta^3}\mathrm{Im}\varepsilon + \ldots. \tag{59}$$

Figure 6 shows $w_\perp(h)$ for $\varepsilon_1 = 5$ and $\varepsilon = 0.1 * i$. This is the solid curve, obtained by numerical integration. The dashed curve is the approximation by the term shown on the right-hand side of Equation (58). We see from the graph that this approximation is excellent for small values of h. This also shows that $w_\perp(h)$ will always be dominated by this diverging term for β small, no matter how small the imaginary part of ε is. For decreasing values of $\mathrm{Im}\varepsilon$, the curve moves closer to the vertical axis, but only for $\mathrm{Im}\varepsilon \equiv 0$ do we get $w_\perp(0) = 0$, as in Figure 3.

10. Conclusions

The power emitted by an electric dipole embedded in a medium is given by P_s in Equation (11). When an interface is present, some radiation is reflected back to the dipole, and this gives an induced power emission P_r. The total emitted power P is given by Equation (13) in terms of the functions $w_\perp(h)$ and $w_{||}(h)$ from Equations (14) and (15). These functions depend explicitly on the dimensionless distance h between the dipole and the interface, and implicitly on the material parameters of the medium through the Fresnel reflection coefficients R_s and R_p for s and p polarized plane waves, respectively. It is advantageous to split these functions in contributions from travelling and evanescent incident plane waves, as shown in Section 4. Then the singularity $1/v_1$ can be removed by appropriate changes of variables. Also, when considering the total power transmitted through the interface, only the evanescent parts of $w_\perp(h)$ and $w_{||}(h)$ contribute, as shown in Equation (34).

The functions $w_\perp(h)$ and $w_{||}(h)$ can be obtained in closed form for an $\varepsilon = 0$ interface, as shown in Section 6. Only the travelling parts of these functions contribute to the power emission, and the total power crossing the interface is zero. In Section 9, we have shown that even the smallest imaginary part in ε of an ENZ material leads to a diverging behaviour of the power when the distance between the dipole and the surface becomes small. This is due to the contribution from the evanescent waves, which is zero for a material with ε identically equal to zero.

Disclosure statement

No potential conflict of interest was reported by the authors.

References

(1) Goy, P.; Raimond, J.M.; Gross, M.; Haroche, S. *Phys. Rev. Lett.* **1983**, *50*, 1903–1906.
(2) Hulet, R.G.; Hilfer, E.S.; Kleppner, D. *Phys. Rev. Lett.* **1985**, *55*, 2137–2140.
(3) Drexhage, K.H. *Progress in Optics*, North Holland: Amsterdam, 1974; pp 163–232.
(4) Chance, R.R.; Prock, A.; Silbey, R. *Adv. Chem. Phys.* **1978,** *39*, 1–65.
(5) Ford, G.W.; Weber, W.H. *Phys. Rep.* **1984,** *113*, 195–287.
(6) Sipe, J.E. *Surf. Sci.* **1981,** *105*, 489–504.
(7) Novotny, L. *J. Opt. Soc. Am. A* **1997,** *14*, 91–104.
(8) Sullivan, K.G.; Hall, D.G. *J. Opt. Soc. Am. B* **1997,** *14*, 1149–1159.
(9) Sullivan, K.G.; Hall, D.G. *J. Opt. Soc. Am. B* **1997,** *14*, 1160–1166.
(10) Holland, W.R.; Hall, D.G. *Phys. Rev. Lett.* **1984,** *52*, 1041–1044.
(11) Grunlke, R.W.; Holland, W.R.; Hall, D.G. *Phys. Rev. Lett.* **1986,** *56*, 2838–2841.
(12) Holland, W.R.; Hall, D.G. *Opt. Lett.* **1985,** *10*, 414–416.
(13) Jackson, J.D. *Classical Electrodynamics*, 3rd ed.; Wiley: New York, 1998; p. 412.
(14) Novotny, L.; Hecht, B. *Principles of Nano-optics*; Cambridge University Press: Cambridge, 2007.
(15) Edwards, B.; Alù, A.; Young, M.E.; Silveirinha, M.G.; Engheta, N. *Phys. Rev. Lett.* **2008,** *100*, 033903(4).
(16) Lobato-Morales, H.; Murthy, D.V.B.; Corona-Chávez, A.; Olvera-Cervantes, J.L.; Guerrero-Ojeda, L.G. *IEEE Trans. Microw. Theory Tech.* **2011,** *59*, 1863–1868.
(17) Torres, V.; Orazbayev, B.; Pacheco-Peña, V.; Teniente, J.; Beruete, M.; Navarro-Cía, M.; Ayza, M.S.; Engheta, N. *IEEE Trans. Antennas Propag.* **2015,** *63*, 231–239.
(18) Massaouti, M.; Basharin, A.A.; Kafesaki, M.; Acosta, M.F.; Merino, R.I.; Orera, V.M.; Economou, E.N.; Soukoulis, C.M.; Tzortzakis, S. *Opt. Lett.* **2013,** *38*, 1140–1142.
(19) Pacheco-Peña, V.; Engheta, N.; Kuznetsov, S.; Gentselev, A.; Beruete, M. *Phys. Rev. App.* **2017,** *8*, 034036(10).
(20) Schwartz, B.T.; Piestun, R. *J. Opt. Soc. Am. B* **2003,** *20*, 2448–2453.
(21) Maas, R.; Parsons, J.; Engheta, N.; Polma, A. *Nat. Photon.* **2013,** *7*, 907–912.
(22) Vesseur, E.J.R.; Coenen, T.; Caglayan, H.; Engheta, N.; Polman, A. *Phys. Rev. Lett.* **2013,** *110*, 013902(5).
(23) Xu, Z.; Arnoldus, H.F. *OSA Contin.* **2019,** *2*, 722–735.
(24) Silveirinha, M.G.; Engheta, N. *Phys. Rev. Lett.* **2006,** *97*, 157403(4).
(25) Silveirinha, M.G.; Engheta, N. *Phys. Rev. B* **2007,** *76*, 245109(17).
(26) Alù, A.; Engheta, N. *Phys. Rev. B* **2008,** *78* (3), 035440(6).
(27) Powell, D.A.; Alù, A.; Edwards, B.; Vakil, A.; Kivshar, Y.S.; Engheta, N. *Phys. Rev. B* **2009,** *79*, 245135(5).

(28) Edwards, B.; Alù, A.; Silveirinha, M.G.; Engheta, N. *J. Appl. Phys.* **2009,** *105*, 044905(4).
(29) Alù, A.; Engheta, N. *IEEE Trans. Antennas Propag.* **2010,** *58*, 328–339.
(30) Enoch, S.; Tayeb, G.; Sabouroux, P.; Guérin, N.; Vincent, P. *Phys. Rev. Lett.* **2002,** *89*, 213902(4).
(31) Alù, A.; Silveirinha, M.G.; Salandrino, A.; Engheta, N. *Phys. Rev. B* **2007,** *75*, 155410(13).
(32) Wang, B.; Huang, K.-M. *Progr. Electr. Res.* **2010,** *106*, 107–119.
(33) Alekseyev, L.V.; Narimanov, E.E.; Tumkur, T.; Li, H.; Barnakov, Y.A.; Noginov, M.A. *Appl. Phys. Lett.* **2010,** *97*, 131107(3).
(34) Girón-Sedas, J.A.; Mejía-Salazar, J.R.; Granade, J.C.; Oliveira, O.N. *Phys. Rev. B* **2016,** *94*, 245430(5).
(35) Rodríguez-Fortuño, F.J.; Picardi, M.F.; Zayats, A.V. *Phys. Rev. B* **2018,** *97*, 205401(9).
(36) Rodríguez-Fortuño, F.J.; Vakil, A.; Engheta, N. *Phys. Rev. Lett.* **2014,** *112*, 033902(5).
(37) Arnoldus, H.F.; Xu, Z. *J. Opt. Soc. Am. B* **2019,** *36*, F18–F24.
(38) Lovat, G.; Burghignoli, P.; Capolino, F.; Jackson, D.R.; Wilton, D.R. *IEEE Trans. Ant.* **2006,** *54*, 1017–1030.
(39) Rocco, D.; Vincenti, M.A.; De Angelis, C. *Appl. Sci.* **2018,** *8*, 2212(10).
(40) Arnoldus, H.F.; Berg, M.J. *J. Mod. Opt.* **2015,** *62*, 244–254.
(41) Arnoldus, H.F.; Berg, M.J.; Li, X. *Phys. Lett. A* **2014,** *378*, 755–759.